Journal of Circuits, Systems, and Computers
Vol. 28, No. 1 (2019) 1950005 (22 pages)

DOI: 10.1142/S0218126619500051

World Scientific
www.worldscientific.com

Comparative Efficiency and Power Assessment of Optical Photoconductive Material-Based Terahertz Sources for Wireless Communication Systems*

Ayhan Yazgan†

Department of Electrical and Electronics Engineering, Karadeniz Technical University, 61080 Trabzon, Turkey
†*ayhanyazgan@ktu.edu.tr*

Lluis Jofre‡ and Jordi Romeu§

Department of Signal Theory and Communications, Universtitat Politecnica de Catalunya, 08034 Barcelona, Spain
‡*jofre@tsc.upc.edu*
§*romeu@tsc.upc.edu*

Received 27 October 2017
Accepted 16 March 2018
Published

Terahertz band has recently attracted the attention of the communication society due to its huge bandwidth and very high-speed wireless communications capability. It has been utilized in a variety of disciplines including physics, biology and astronomy for years; and the main concerns have always been obtaining highly efficient and high-power terahertz sources. Today, these problems are still the most important issues in establishing an operable wireless terahertz communication link. In this paper, recent studies in the field of terahertz source design are investigated based on the terahertz output power and efficiency. Solid-state sources and optical sources were comparatively reviewed with optical photoconductive material (OPM)-based methods which were combined with the terahertz antennas in the design phase generally. For wireless communication, the most suitable frequencies are between 0.3 THz and 1 THz due to the attenuation profile of the atmosphere. For this reason, based on the recently published studies, it has been observed that OPM and resonant tunneling diode-based sources are the most promising terahertz sources in terms of efficiency and power. Key issues and the main problems of terahertz photoconductive antennas which are the base of OPM method were also discussed in this paper.

Keywords: Efficient terahertz source; terahertz power; CMOS; HBT; QCL; RTD; OPM; optical photoconductive material-based antennas; wireless terahertz communications.

*This paper was recommended by Regional Editor Piero Malcovati.
†Corresponding author.

1. Introduction

Limited spectral efficiency is one of the major obstacles in achieving a reliable high-speed wireless communication link. As an example, LTE peak data rates are around 1 Gb/s and 60-GHz systems offer 10 Gb/s which is still at least two orders of magnitude below the Tb/s data rates. Considering an infrared (IR) transmission system which has been proposed for wireless local area networks, even in the presence of line-of-sight (LOS), it is still hard to reach very high-speed communication links due to the high propagation losses and poor sensitivity of receivers. The data rate can reach 10 Gb/s under LOS conditions and yet it is still two orders of magnitude below the Tb/s data rates. Another disadvantage of the IR band is that it is not feasible to use high-power sources for health reasons (eye safety limitations).[1] Due to its many advantages reported several times, the interest in terahertz band, which lies between microwave and infrared, is increasing day by day in a variety of science disciplines including physics, chemistry, biology, astronomy and engineering. Especially, terahertz spectrum is a very promising part of the electromagnetic spectrum for the use in space applications, spectroscopy and different kinds of imaging applications such as medical and security. Nowadays, it is found to be very crucial for high-speed wireless communication systems. Although it offers a large bandwidth, there are many issues which are still on the table to be dealt with such as determining the optimum carrier frequency and designing efficient terahertz sources. As mentioned above, the frequency band can change the communication performance in terms of atmospheric effects. According to the reported studies, the terahertz frequency band has been identified in different ranges of operation. The reason may be due to the absence of published standards except by some workgroups such as the IEEE 802.15 Terahertz Interest Group. Therefore in Ref. 2, the terahertz communication band is reported between 0.275 THz and 1 THz. In another study, authors define the terahertz band between 0.1 THz and 2 THz.[3] The terahertz band is defined and studied from 0.3 THz to 3 THz both in Refs. 4 and 5. In another two studies, the terahertz bandwidth varies between 0.3 THz and 10 THz and between 0.1 THz and 10 THz.[6,7] In Refs. 8 and 9, the band is further extended and is defined between 0.1 THz and 30 THz. Although there is a wide spectrum available on the high-frequency side of the terahertz band, in spite of the high atmospheric attenuation in the bands from 1 THz to 30 THz, it is very reasonable to study in the range of 0.3–1 THz band for the wireless communication link. However, in some special cases, the upper band of the terahertz spectrum (1–30 THz) may also be allocated for wireless indoor communication links. To construct a wireless terahertz communication link, no published standard is available which limits the terahertz power density except for the radio astronomy protection criterion. Due to interference with the terahertz waves coming from space, terahertz sources should not exceed a certain power. Therefore, in the case of outdoor terahertz communication, the system needs to be designed carefully to comply with the rules. As an example, if the transmitter power

is 7 dBm, the link should be 55 km away from the radio telescopes to keep the interference at certain levels.[10] For a wireless terahertz communication system, some of the negative effects of the link budget may be eliminated using higher gain antennas at specific frequencies; but, designing and fabricating an efficient high-power terahertz source, which is a very hot topic today, is another important issue that needs to be focused on. Although many types of terahertz source methods have been reported by far, in this study, most efficient and powerful experimental methods were reviewed and compared with the terahertz antennas-based optical photoconductive material (OPM) method. In the solid-state part of these methods, multiplier chains are utilized in general to reach the terahertz band by increasing the output frequency in each stage. As an example, in a three-stage multiplier, the first stage is composed of Schottky diode device based on GaAs, the second stage is based on two GaAs designs and in the last stage a single unbiased device is inserted to form a tripler device.[11] In case of this multiplier, the output terahertz power and frequency are measured as 0.014 mW and 2.58 THz, respectively.[11] As expected, in the lower band of the spectrum, solid-state devices perform better in terahertz region. For example, in a reported study, solid-state impact avalanche and transit time diodes have been used for 0.11-THz source design and 2.82-mW output power is reported.[12] Conversely, quantum cascade lasers (QCLs) perform better at higher frequencies of terahertz band and the output power increases when the signal frequency increases within the terahertz band. These opposing conditions will be discussed in the following sections in this work. Although solid-state-based terahertz sources gradually fill the lower side of the terahertz spectrum, they face a dramatic power decrement ratio which is around $1/f^4$. Therefore, it is very hard with current technology to increase both the output frequency and power of this type of sources.[13] Reported studies have shown that besides solid-state and QCL, in order to form better wireless terahertz communication links, different types of sources are needed to fill the frequency bandgap between solids and QCL. For this reason, several methods have been proposed. Recently, terahertz antennas deposited on OPM have been reported as an alternative terahertz source. These sources can be a good alternative to solid-state and QCL sources in the interested band of the terahertz spectrum (0.275–4 THz). Researchers have been trying to increase the efficiency and output power of these new terahertz sources; they recently have proposed utilizing of three-dimensional plasmonic contact electrodes and have reached an efficiency of up to 7.5%.[14] As new methods are likely to bring new problems, in this structure, they have faced a power limitation due to the screening effect which will be discussed in next section. Basically, there are two main options in the OPM method to configure the terahertz sources; continuous wave (CW) terahertz radiation using a photomixer and pulsed terahertz radiation using a femtosecond (fs) laser. Both methods will be discussed in the following sections. Additionally, various types of terahertz sources such as gyrotron, cyclotron and vacuum electronics have also been reported to obtain a high-power

terahertz source.[15–17] Even if these sources provide high output powers, generally in the kW region, they need huge magnetic and electric fields which make them too bulky and inefficient. For this reason, these devices are not considered from a communication point of view. Significant review papers have been published in literature so far.[1–10,18] In this review, we concentrated on and discussed different kinds of terahertz sources mostly published within the last four years and proved by experimental studies. Additionally, potentially efficient source methods for a wireless terahertz communication link are discussed and the principle of the OPM method is given in detail. A preliminary version of this paper has been presented at the *2017 40th International Conference on Telecommunications and Signal Processing* (TSP).[19] In this paper, powers and efficiencies are not normalized and the real values are given in the respective tables and the figures.

In Sec. 2, the recent advancements in complementary metal oxide semiconductor (CMOS), heterojunction bipolar transistor (HBT), resonant tunneling diode (RTD), OPM and QCL methods are given. Since it is the main focus of this paper, the OPM method is discussed more in detail than the other methods. In Sec. 3, the challenges to wireless terahertz communications and recent studies were given. In this section, we discussed and compared all methods together. Section 4 concludes the paper.

2. Terahertz Sources

The necessity of using high-frequency bands increases due to the rise of technology usage in daily life. Therefore, terahertz technology becomes a hot topic nowadays in several research fields which utilize different properties of terahertz spectrum. Absorption is an example which is very important property and is desired in terahertz spectroscopy to characterize the material under test. On the other hand, absorption is one of the important transmission parameters of wireless terahertz communication. However, it is unfavorable especially for long link distances. Since we focus on terahertz communication, in this paper, we mostly consider the possible compact and efficient sources. The aforementioned terahertz source methods are discussed in this section from the points of view of output power, operating frequency, efficiency and temperature. The ambient temperature is the room temperature when not specified on the tables. Additionally, the output terahertz powers given in the tables are the maximum output powers within the related frequency band.

2.1. *Complementary metal oxide semiconductor*

CMOS has been used in electronic designs for years because of its significant advantages such as low power consumption and low heat sinking in digital and analog electronic circuits. Recently, high-frequency operation capability of CMOS offers alternative solutions in the lower band of the terahertz spectrum. In high-frequency (lower terahertz band) applications, a voltage controlled oscillator (VCO)

Table 1. Recent CMOS studies and their results.

Study	Frequency (THz)	Output power (mW)	EIRP (dBm)	DC to RF efficiency (%)	Published year
Ref. 20	0.288	1.000	10.2	0.3400	2015
Ref. 21	0.288	0.389	—	0.1400	2013
Ref. 22	0.293	0.537	6.4	2.7900	2014
Ref. 23	0.380	0.398	8	0.5300	2016
Ref. 24	0.320	0.575	10.6	0.0575	2015
Ref. 25	0.300	1.250	—	0.5100	2016
Ref. 26	0.256	2.600	—	1.4000	2014
Ref. 27	0.498	0.022	—	0.0051	2015

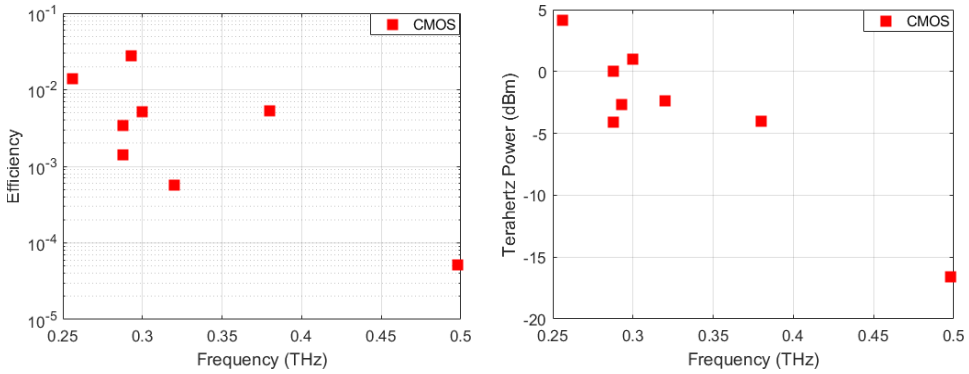

Fig. 1. The output powers and efficiencies from recent CMOS studies.

or an active multiplier chain is inserted in the CMOS device.[20] In some of the studies based on the CMOS technology, authors combine the CMOS chip and antennas together and report the EIRP values. In some publications, only the EIRP values are given. To perform a fair comparison, we subtracted the antenna gain and obtained the pure CMOS output power. Additionally, the EIRP values are also given in Table 1. In Refs. 20–27 output powers from 22 μW to 2.6 mW between 0.288 THz and 0.498 THz are reported. Generally, different triplers are used to multiply the frequency from X-band to lower terahertz band using nanometer CMOS technology. In these studies, maximum efficiency, output power and frequency are measured as 2.79%, 2.6 mW and 0.498 THz, respectively. According to the results, when the output power is high, the efficiency and the operating frequency are low, as expected. In order to obtain high-power and high-frequency efficient CMOS devices, a constructive addition of harmonic signals is required instead of multiplier chains, but the losses of the combiners should be minimized. Moreover, this technology may also be combined with several different technologies and the output power and operating frequency may be increased. Reviewed studies in Refs. 20–27 are given comparatively in Table 1 and Fig. 1.

2.2. *Heterojunction bipolar transistor*

To include the Si-based technologies into terahertz systems, researchers combine silicon and germanium to obtain relatively smaller bandgap SiGe alloys.[28] The applicability of SiGe alloys opens a new design path which has been unavailable in Si technology so far.[28] Besides SiGe alloys, InP or different alloys may also be used to construct the HBT technology. Comparing with CMOS, higher frequency sources with higher output powers are reported. In HBT technology, recent studies concentrate on power combining structures instead of multiplier chains or amplifiers. Recent reported results, from 12 μW to 10 mW at 0.215–0.92 THz bands, have been reviewed where the efficiencies are between 0.01% and 5.1%. Some of the reported results[29–37] are given in Table 2 and plotted in Fig. 2.

Table 2. Recent HBT studies and their results.

Study	Frequency (THz)	Output power (mW)	EIRP (dBm)	DC to RF Efficiency (%)	Published year
Ref. 29	0.276	10.00	—	5.1000	2017
Ref. 30	0.248	4.266	—	1.3000	2016
Ref. 31	0.215	6.309	—	—	2016
Ref. 32	0.320	1.445	—	0.7000	2015
Ref. 33	0.320	3.3	22.5	0.5400	2015
Ref. 34	0.92	0.0186	−10	0.3263	2017
Ref. 35	0.573	0.0120	—	0.0104	2011
Ref. 36	0.316	4.2	—	3.2000	2014
Ref. 37	0.3058	3.388	—	3.9000	2017

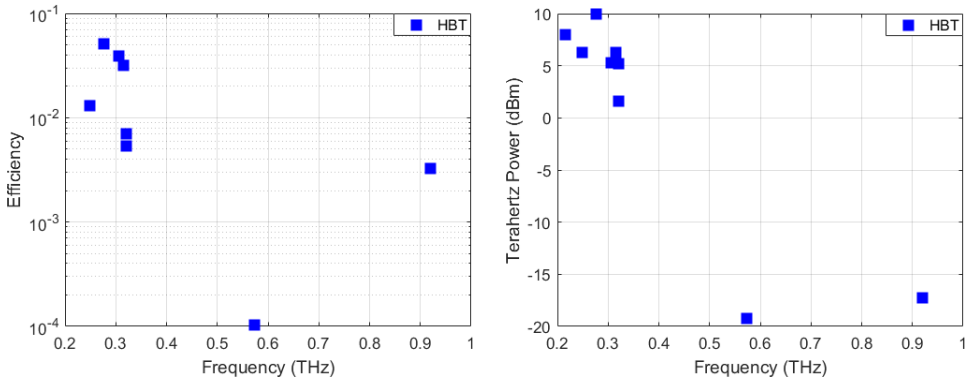

Fig. 2. Recently reported results of HBT output powers and efficiencies.

2.3. *Quantum cascade lasers*

As a general rule based on the well-known Planck's equation, the bandgap of the material determines the output wavelength or frequency of the laser. The bandgap

energy of the material becomes very small in terahertz region according to the Planck's equation. This result brings a significant problem to build a terahertz laser in the construction side, especially in lower band of the spectrum. The lack of suitable materials which satisfy the Planck's equation limits the output frequency to access the lower parts of the terahertz band. Therefore, QCLs are proposed with a different structure to operate inside the terahertz band. Indeed, QCLs are semiconductor lasers with an advantage of having the capability of inter subband transitions. In classical lasers, the photon is emitted when the electron–hole recombination occurs. On the other hand, in QCLs, the semiconductor layers are very thin and low-energy transitions may happen when electron tunnels from one layer to another. Since the energy is quite low, the emitted radiation occurs in terahertz region. Recent years, down to 1-THz output frequencies have been obtained by utilizing cooling mechanisms. Thanks to the lower operating temperature, higher wavelengths can be obtained. However, cooled QCL consumes huge powers and therefore very low efficiencies are faced especially below 1 THz. Additionally, these cooling devices are bulky as well. Therefore, for now, quantum cascade laser-based terahertz sources are not suitable for the lower band of the terahertz spectrum which is very important for wireless terahertz communication as discussed above. Besides, even if the atmospheric attenuation is very high, QCLs may be an alternative source for wireless communication links at the upper band of terahertz spectrum. There are some studies which report QCLs operating at 1-THz region, but their efficiencies are quite low because of the power consumption of cooling mechanism.[38] Recently reported studies[39–41,43–46] are given in Table 3 and Fig. 3. Note that the cooled QCL studies (QCLc) are illustrated using asterisk to separate them from room-temperature QCL (QCLr) studies. Differently, in Ref. 42, phase-locking of a THz quantum cascade laser is proposed to obtain an accurate and stable local oscillator to design a terahertz receiver. The frequencies are given where the maximum output power is obtained. The efficiency is not given in QCL studies and it is not listed in Table 3 because the cooling mechanisms consume different power for each study.

Table 3. Recent QCL studies and their results.

Study	Frequency (THz)	Output power (mW)	Temperature (K)	Published year
Ref. 39	1.9	0.04	293	2017
Ref. 40	3.41/2.06	0.014/0.0006	293	2016
Ref. 41	3.57	0.080	293	2016
Ref. 43	3.1	1	—	2010
Ref. 44	3.4	1,010	10	2014
Ref. 45	3.87	—	120	2017
Ref. 46	3.4	103	20	2012

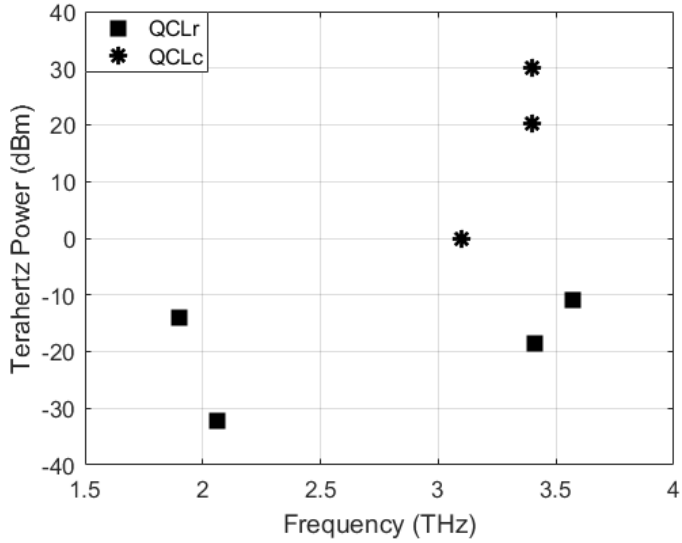

Fig. 3. QCL output powers from recent studies in the literature.

2.4. *Resonant tunneling diode*

Resonant tunneling diodes have been utilized in terahertz applications since the ordinary transistors became insufficient for high-speed applications. Normally, current flows through the channel between the drain and source in conventional transistors. Whereas, in tunneling diodes, current passes the depletion region directly, and this is known as "tunneling process". In the physical design, tunneling diodes are composed of highly-doped p- and n- junctions with a very narrow depletion region. Since the depletion region is on the nanoscale, electrons may tunnel easily and produce a forward current. Considering classical physics, it is impossible to pass across the energy barrier without any additional energy. On the other hand, in quantum physics, matter may act as a wave. This situation is a solution of Schrödinger's wave equation. Therefore, in quantum physics, according to the wave theory, if the barrier is thin enough, an electron may tunnel through to the barrier at certain energy levels and can pass through to the other side without any need of additional energy such as QCL. This is the basic phenomenon of the tunnel or (Leo Esaki) diodes. In RTD, there are two barriers and the energy levels are quantized where only electrons having specific energy are able to tunnel. Therefore, tunneling process happens only for the specific energy levels which depend on the doping levels and the depletion region thickness. The tunneling process is very fast and therefore suitable for high-speed applications such as terahertz sources. Recent works on RTDs[47–56] are given in Table 4 and Fig. 4.

Table 4. Recent RTD studies and their results.

Study	Frequency (THz)	Output power (mW)	DC to RF efficiency (%)	Published year
Ref. 47	0.675	0.0470	0.330	2016
Ref. 48	1.52	0.0019	0.016	2016
Ref. 49	0.308	0.3311	0.173	2016
Ref. 50	0.620	0.6100	—	2016
Ref. 51	0.64	0.0010	0.000035	2016
Ref. 52	0.655	0.0050	—	2014
Ref. 53	1.92	0.0004	—	2016
Ref. 54	1.55	0.0004	—	2014
Ref. 55	1.31	0.0010	—	2012
Ref. 56	0.284	0.46	0.184	2017

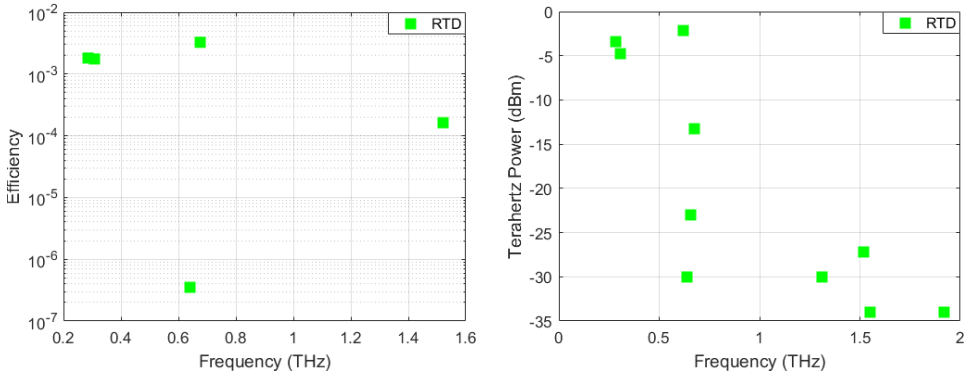

Fig. 4. RTD output powers and efficiencies reported in recent works.

2.5. *Optical photoconductive material*

Since the main focus of this paper is to compare the OPM method with other methods, the basic concept of OPM method will be discussed here in more detail. The pulsed and photomixing methods are given with operational difficulties in reaching high power and efficiency. There are basically two different OPM methods in terahertz sources. Both methods use photoconductive antennas to emit the terahertz radiation. One of them is the pulsed method which uses only one pulsed laser to illuminate the semiconductor and gives rise to terahertz emission. The second one is the photomixing method. In photomixing case, two adjacent lasers illuminate the semiconductor and produce CW terahertz emission.

2.5.1. *Pulsed OPM*

In order to obtain terahertz power using pulsed method, a femtosecond laser is utilized to emit ultrashort optical pulses. A short carrier lifetime is needed to obtain high terahertz power. Since its carrier lifetime is around 200–400 fs, low-temperature-grown

GaAs is used generally as a semiconductor material. Due to the applied optical short pulses by the femtosecond laser, carrier generation occurs in the semiconductor material. Meanwhile, a DC bias is also applied to accelerate the electron–hole pairs on the semiconductor surface. The transit time of the photocarriers is one of the key parameters to achieve terahertz radiation[14] which is emitted on the back side of the semiconductor by a terahertz antenna connected to the metallic electrodes. This terahertz antenna is fed by the produced terahertz signal on the semiconductor surface. The type or dimension of the terahertz antenna is determined by the operation purpose and frequency, respectively.

Semiconductor conductivity σ which is related to the radiation is calculated as given in Eq. (1):

$$\sigma = qn_e\mu_e + qn_p\mu_p\,, \tag{1}$$

where q is the electron charge, n_e and n_p are electron and hole concentrations and μ_e and μ_p are electron and hole mobilities, respectively. The surface current density $J(t)$ is defined as given below where v_e and v_p are the drift velocities[18]:

$$J(t) = qn_e v_e + qn_p v_p. \tag{2}$$

Due to the drift velocity being a multiplication of mobility and applied bias field, the optical illumination and applied bias field are responsible together for the terahertz radiation. Using the equations above, the terahertz far-field can be obtained as in (3) and (4) where A is the radiating surface area, c is the speed of light in free space, ε_0 is vacuum permittivity, n is the total concentration of carriers, z is the distance from source and v is carrier velocity[18]:

$$E(z,t) = -\frac{A}{4\pi\varepsilon_0 c^2 z}\frac{dJ}{dt}\,, \tag{3}$$

$$E(z,t) = -\frac{A}{4\pi\varepsilon_0 c^2 z}\left(qv\frac{dn}{dt} + qn\frac{dv}{dt}\right). \tag{4}$$

2.5.2. *Photomixing*

Thanks to its continuous wave output capability, photomixing method may be more attractive than the pulsed method from the point of view of wireless terahertz communication. As described before, photomixing method needs two continuous laser beams with a wavelength difference related to the terahertz spectrum. Assuming the two laser beams have intensities I_1 and I_2 at frequencies f_1 and f_2, respectively, the intensity $I(t)$ at the semiconductor surface is given in (5):

$$I(t) = I_1 + I_2 + 2\sqrt{I_1 I_2}(\cos 2\pi(f_1 - f_2)t + \cos 2\pi(f_1 + f_2)t)\,. \tag{5}$$

The term $\cos 2\pi(f_1 - f_2)t$ is responsible for the terahertz radiation in photomixing method. Like in the pulsed system, the terahertz far-field is directly related to the

time derivation of the surface current density. A DC bias is also applied to accelerate the electron-hole pairs in the same way as in the pulsed method.

The THz radiation using OPM method is not restricted to a single frequency. Most studies given here cover some parts of the THz band. Therefore, for some literature results in Table 5, related efficiencies and powers are given for frequency bands instead of a single frequency. The most recent literatures about pulsed and photomixing optical methods are given in Table 5. In Ref. 57, plasmonic nanoantennas are used and high dipole moment is obtained. GaAs is used as a photoconductive material which has a carrier lifetime of 0.3 ps. The efficiency is obtained as 1.58% for the pulsed THz radiation. In Ref. 14, authors used 3D plasmonic electrodes and obtained a world record high efficiency of 7.5%. They used LT GaAs as a photoconductive material with 400-fs carrier lifetime. The disadvantage of this structure is the presence of power limitation because of screening effect where the produced carriers screen the applied DC field and therefore saturate the output THz radiation. In Ref. 58, a continuous THz signal is produced by investigating the effect of size of the nanogrid on the THz power radiation. It is shown that the power of THz signal increases with smaller nanogrid structures. In Ref. 59, for continuous THz radiation, bimodal lasers are used. The efficiency is measured as 0.18% which is still fair for a photomixing operation. A comparison between the plasmonic and conventional contacts is reported in Ref. 60. It is emphasized that using plasmonic contacts gives 50 times higher terahertz radiation power than conventional ones. In Ref. 61, the radiation frequency is tuned by varying the angle of the incident optical excitation. The efficiency is measured as 0.001%. In Ref. 62, vertical external cavity surface emitting laser (VECSEL) which can emit dual wavelength simultaneously by intracavity filter is used. In this study, 2-mW THz power at 1.9 THz is reported. One of the important ways to increase the THz power is to increase the optical near-field in the semiconductor. In Ref. 63, three kinds of electrodes are proposed, and it is determined that the bias field distribution is important to obtain higher THz power as well. In Ref. 64, several parameters such as DC bias voltage, antenna impedance and gap have been varied in order to reach maximum efficiency. The efficiency is reported as 0.0269%. In Ref. 65, plasmonic contact electrodes are used to obtain an efficient photomixer and 17 μW THz power is reported. In Ref. 66, 1,550-nm optical wavelength power source is used, and 0.3-mW THz power is reported.

Now it is well known that the plasmonic contact electrodes increase the optical to terahertz conversion efficiency and power. The contact electrodes can concentrate the incident optical radiation in the vicinity of electrodes and therefore the average transport path length of the produced carriers is reduced, and this increases the photocarriers whose drift is responsible for the terahertz radiation. In Ref. 67, authors report a novel technique to further increase the efficiency and power of the proposed OPM-based terahertz source. To make an efficient stick process between Au and semiconductor, an adhesion layer base (chromium) is proposed.

Table 5. Recent OPM studies and their results.

Study	Frequency (THz)	Output power (mW)	Type	Efficiency (%)	Published year
Ref. 57	0.1–5	3.8	Pulsed 2D plasmonic	1.58	2015
Ref. 14	0.1–2	0.108	Pulsed 3D plasmonic	7.5	2014
Ref. 58	0.4	0.1	Plasmonic photomixer	0.11	2012
Ref. 59	1.62	0.45	Plasmonic photomixer	0.18	2016
Ref. 61	0.65–1.4	0.008	Optical rectification	0.001	2008
Ref. 62	1.9	2	IR to THz	0.0042	2011
Ref. 64	—	0.5	Pulsed	0.0269	2013
Ref. 65	1	0.017	Plasmonic photomixer	0.113	2016
Ref. 66	0.1–5	0.3	Pulsed	0.075	2016
Ref. 67	0.1–4	6.7	Pulsed 2D	0.96	2017
Ref. 68	0.1–4	4	Pulsed 3D	0.55	2017

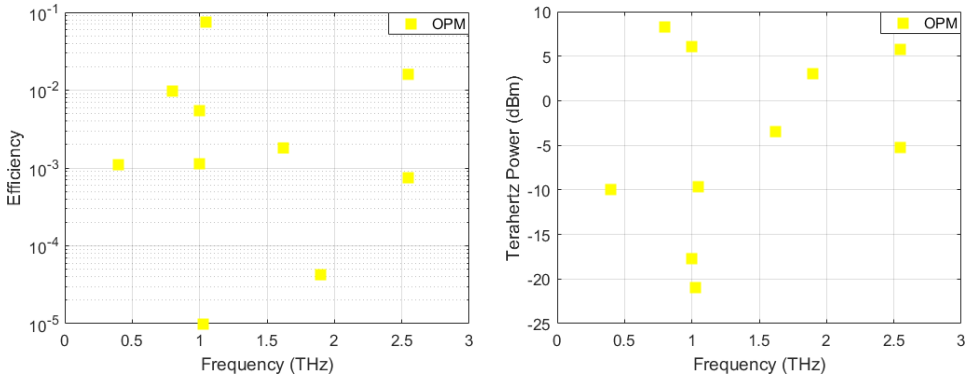

Fig. 5. Recent OPM output powers and efficiencies reported in literature.

Using this technique, they reach 6.7-mW terahertz power applying 700-mW optical power which points to a good efficiency. Using distributed Bragg reflector-based nanocavity, authors have achieved strong confinement of the optical beam and 4-mW terahertz power is reported in Ref. 68. In order to see the differences clearly, reported results of recent OPM studies are summarized in Table 5 and plotted in Fig. 5.

Terahertz communication researchers try to obtain higher terahertz source efficiency and output power in tandem, but this is not always the case. Note that the maximum efficiency does not always cause the maximum power output. This issue will be discussed in the following sub-subsection. According to the recent results, maximum efficiency is reported in Ref. 14 and the maximum power is reported in Ref. 67.

2.5.3. *Key issues in terahertz photoconductive antenna designs*

Since the initial observations of electromagnetic radiation in the THz frequency range in photoconductive antennas excited by continuous wave lasers or by ultra-fast laser pulses, considerable efforts[69] have been made to understand the mechanisms

responsible for the THz generations and more importantly their basic limitations and the corresponding low efficiencies. Different analytical approaches and experimental studies have been conducted to address these challenges. Based on these studies, some basic strategies to address these issues may be pointed out.

(a) *The screening effect*: Recent experimental studies[70] using the pump and probe THz generation technique[71] propose that the field screening effects produced from the separation of the electrons and holes may result from two basic phenomena:

(1) The space-charge effect (E_{sc}), due to the applied bias (E_{bs}), more significant in the case of continuous wave emitters.
(2) The effect due to the local (impressed) field created by the THz radiation (E_{rd}) more significant for low-repetition-rate pulses. The local electric field in the gap may be then written as given in (6):

$$E(t) = E_{\text{bs}} - E_{\text{rd}} - E_{\text{sc}}. \tag{6}$$

Results for the antenna temporal response seem to indicate that in the initial time the radiation field produced by the THz radiation is much larger than the space-charge field created by the bias voltage, and so the impressed (gap) radiation field screening dominates the early response of the device. Results also show that the impressed radiation field decreases with an increasing gap dimension (d) and therefore, the peak of the radiated THz field is larger. A basic conclusion here will be the interest on investigating antennas that may obtain simultaneously a low input impedance, resulting from the combined effects of a short gap distance d with a longer width w, and the increase of the electrodes exchanging dimension when co-incident with w. On the other hand, screening effects have also been shown to occur only $\sim$0.5 ps after the irradiation that may represent traveling distances below μm for the photoexcited electrons or holes.

(b) *Photocarrier velocities*: In general, each photocarrier is generated with zero or near-zero velocity and is then accelerated for a certain time during which velocity increases to a maximum value that depends on the carrier type, the specific semiconductor and the temperature.[72] Each photocarrier can be associated with a transit length and an average velocity, resulting in a transit time that must be compared with its corresponding average lifetime. The objective would be to have a transit time as reduced as possible with respect to its average lifetime, for which it would be of great interest to enter the active area with a certain initial velocity different from zero. Here the idea would be to use discrete plasmonic nanoantenna elements[73] to concentrate as much as possible the active area in such a way that when the carriers that have been previously accelerated up to a certain high average velocity enter this limited area, it allows them to navigate through this irradiated area with a reduced transit time in terms of their average lifetime thereby maximizing the THz signal generation.

(c) *Optical footprint reduction*: While the use of nanoantennas has allowed for the concentration of illuminating optical field in areas with dimensions of a small fraction

of optical wavelengths (tens of nanometers) and thereby cause an increase in the intensity of the irradiating field and as a consequence the generation of photocarriers, from the point of view of the efficiency of the whole system, the enhanced optical area occupies just a small part of the optical footprint that according to the diffraction limits would be in the order of a circle of diameter close to the wavelength (hundreds of nanometers). As a result, just a small fraction of the total illuminating optical power has actually been used with the corresponding impact in terms of efficiency. In order to avoid this inefficiency, there could be the possibility of trying to concentrate the illuminating field using a subdiffraction-limiting technique using either a transmission line technique with a line cross-section matching the illumination requirements or a near-field high-resolution focusing technique[74] producing an illumination footprint coincident with the reduced active area. For the first case, solutions based on metamaterial geometries[75] may be extended to three dimensions to build sub diffraction transmission lines. In the second case different types of subdiffraction lenses[76] may be alternatively designed. Depending on the specific technique, different focusing effects may be obtained, but focusing regions well below the wavelength (i.e., $\lambda/28$)[77] have already been demonstrated.

3. Discussion

Recently, wireless terahertz communication has attracted more attention of researchers in communication society because of its huge bandwidth and high-speed communication capability. On the other hand, there are many difficulties to realize a high-speed wireless terahertz communication link such as modulation schemes, propagation modeling and capacity analysis.[7] Some communication modules have already been reported, such as terahertz modulation, demodulation and channel measurements.[7–10]

In a simple terahertz communication system, basically, transmitter and receiver modules are needed for communication. When it is designed for communication purposes, the type of terahertz source may become an important issue considering the compactness and efficiency. Therefore, semiconductor-based sources are more appropriate for communication purposes. In Ref. 78, authors report a frequency multiplexer at 10 Gbit/s, and they demonstrate two simultaneous signals at different carrier frequencies, with an aggregate data rate of 50 Gbit/s. In Ref. 79, a wideband 2×2 cavity-backed slot antenna array with a corrugated surface is proposed. They integrated a series-resonant electric dipole with a parallel-resonant magnetic dipole where slots work as magnetic dipoles and the corrugated surface radiates as an array of electric dipoles at 1 THz. Their fractional gain and bandwidth are reported as 14 dBi and 26%, respectively. In Ref. 80, a quantum cascade laser is modulated by 6.2-GHz signal and detected by a quantum well photodetector. In Ref. 81, authors design a modulator and a demodulator for a quantum cascade laser using graphene-based materials. An antenna beam steering is also reported in Ref. 82. Using 1-THz

region, $1,024 \times 1,024$ ultra massive MIMO system is proposed for very high-speed wireless terahertz communication systems.[83] Authors use plasmonic optical nanoantennas for beamforming properties.

Since communication is a new topic for terahertz researchers, many types of transmitter and receiver designs are still in research phase now. Researchers also make great effort to deliver their experience and methods from microwave to terahertz spectrum. It is clear that the key point that needs to be focused on is to design efficient high-power compact terahertz sources.

Considering the recent studies published so far, when all the results are put together as given in Figs. 6 and 7, the level of terahertz power that can be obtained by the researchers at different frequencies and efficiencies can be seen. Results also show the way in which researchers should go to obtain efficient terahertz transmitters. In general, each method has several advantages and disadvantages compared to each other. Considering the output power which is given in Fig. 6, at low frequencies CMOS is the best possible terahertz power source. However, the output power of CMOS and HBT decreases dramatically above 0.3 THz. On the other hand, QCL may be a good alternative above 2 THz but it cannot reach below 1-THz region even if the cooling temperature reaches near absolute zero. In addition, cooling systems are too bulky and not efficient for terahertz communication. It can be seen from Fig. 6 that the RTD and OPM are the best methods with respect to the output power values between 0.5 THz and 3 THz. For the efficiency discussed in Fig. 7, the best efficiency results are observed when the OPM method is used to design a terahertz source. However, the efficiency is still lower than 10% and still needs to be improved. Since the power consumed by the environmental units is not certain, QCL efficiency is not given in Fig. 7.

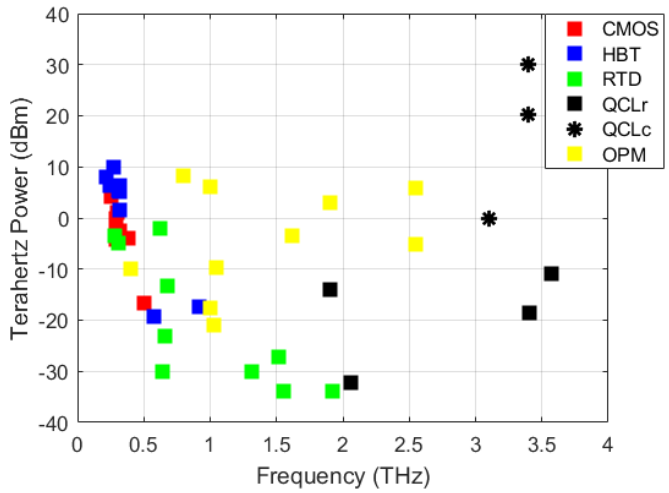

Fig. 6. Output powers of different types of terahertz sources.

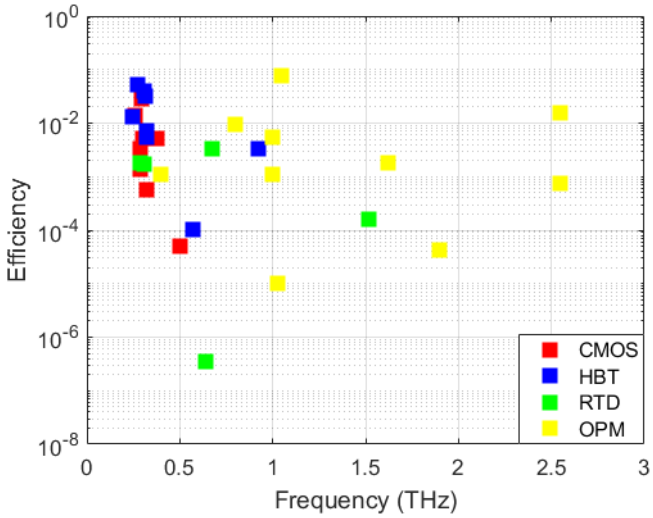

Fig. 7. Efficiencies of different types of terahertz sources.

Different kinds of sources such as impact ionization avalanche transit-time (IMPATT) diode may also be used for terahertz applications. IMPATT diodes are used for high-frequency sources because of the negative resistive properties in high frequencies and high capacitive loads in low-frequency regions.[84] There are some studies that claim high efficiencies (more than 10%) in THz region. However, these studies are not experimentally proven and therefore not included in this review. In experimental studies, mostly silicon or GaAs is used for the sources up to 0.2 THz. Above 0.2 THz, simulation studies up to 1.5 THz can be found where several kinds of materials such as GaN or wurtzite–GaN (Wz–GaN) are used. Another source which is not mentioned in this review is high-electron-mobility transistors (HEMTs). HEMT, which is originally a field effect transistor, is a heterojunction structure composed of a low bandgap material sandwiched between two high bandgap materials where carriers are confined. The confining process gives rise to an electron gas and high mobility. GaAs is a high-electron-mobility material and therefore it is also used in HEMT devices, generally. Mostly AlGaAs/GaAs/AlGaAs or AlN/GaN/AlGaN are formed as the heterostructure because of excellent lattice match. In literature, up to 0.91-THz sources have been recently reported.[85–87]

All recent technologies reported in this paper are commercially available in the open market and the product information can be viewed online. Obviously, the power and the efficiency values in the market are lower than those in the reported academic papers. For example, the *laser quantum Tera-SED* is a pulsed OPM terahertz source operating from 0.1 THz to 7 THz with 0.2% conversion efficiency using a femtosecond laser pulse. The peak power of this device is observed at 1-THz region of the terahertz spectrum. Another commercially available product is from

TeraSense and it produces 10-mW terahertz power at 0.3 THz by using IMPATT technology. The efficiency is not given in reviewed data sheet. *Toptica* offers both photomixer continuous based-wave and femtosecond laser-based pulsed terahertz sources. They use GaAs- and InGaAs-based emitter/receiver modules up to 65-μW output powers at 2 THz for photomixer-based continuous wave products. Using a classical femtosecond laser, for pulsed systems, they can reach up to 5 THz. *Menlo Systems* and *Ekspla* produce terahertz sources generally for spectrometers and imaging applications and the efficiencies and output powers are not provided in reviewed data sheets. From the small commercial review of terahertz sources, consequently, it can be concluded that commercial products on the market focus more on spectrometers and imaging systems than wireless terahertz communication systems. This is due to the fact that the wireless terahertz communication is still a new research area in academic world.

4. Conclusion

In this study, recent studies related to the terahertz sources and communications were studied and reviewed. Considering the output power and efficiency, it can be concluded that the gap between microwave and infrared has already started to be filled by the yellow signs which point to OPM method in the figures. OPM needs the optical pump to illuminate the semiconductor and to obtain accelerated electron–hole pairs. Inserting plasmonic nanoelectrodes into the photoconductive active area increases the optical near-field in the semiconductor and leads to an improvement of the terahertz radiation in terms of both power and efficiency in 2D and 3D semiconductor platforms. Due to the atmospheric effects, the most suitable frequency bandwidth for wireless terahertz communication is 0.3–1 THz. Even though it needs to be further improved, OPM method covers this spectrum with considerable efficiency and power rates. On the other hand, if the communication band is assigned under 0.5 THz, then the CMOS and HBT methods may perform better in this lower terahertz band. It should be noted that RTD method which is proper for subterahertz or terahertz bands, would be a good alternative to OPM method for wireless communication purposes, when necessary. In addition, QCL provides good results in terms of power for 2 THz and above, but its efficiency is very low and needs to be improved. In this paper, we mainly focused on the most recent experimental studies, but the terahertz source concept is still a hot topic and the literature in this area changes very fast. Therefore, we suggest the readers and engineers to be updated with recent developments in this topic. Considering the current and prospective powerful and efficient methods, from this review we can also conclude that 1-Tb/s wireless link is not far away anymore.

Acknowledgments

This work was supported by FEDER and the Spanish Comisión Interministerial de Ciencia y Tecnología (CICYT) under the Projects TEC2013-47360-C3-1-P

and TEC2016-78028-C3-1-P and the Unidad de Excelencia Maria de Maeztu MDM-2016-0600, which is financed by the Agencia Estatal de Investigacion, Spain. We acknowledge funding from Scientific and Technical Research Council of Turkey (TUBITAK, 2219-International Postdoctoral Research Scholarship Program).

References

1. M. Wolf and D. Kress, Short-range wireless infrared transmission: The link buoget compared to RF, *IEEE Wirel. Commun.* **10** (2003) 8–14.
2. T. K. Ostmann and T. Nagatsuma, A review on terahertz communications research, *J. Infrared Millim. Terahertz Waves* **32** (2011) 143–171.
3. J. Federici and L. Moeller, Review of terahertz and subterahertz wireless communications, *J. Appl. Phys.* **107** (2010) 111101.
4. P. H. Siegel, Terahertz technology, *IEEE Trans. Microw. Theory Tech.* **50** (2002) 910–928.
5. P. H. Siegel, Terahertz technology in biology and medicine, *IEEE Trans. Microw. Theory Tech.* **52** (2004) 2438–2447.
6. X. C. Zhang, A. Shkurinov and Y. Zhang, Extreme terahertz science, *Nat. Photonics* **11** (2017) 16–18.
7. I. F. Akyildiz, J. M. Jornet and C. Han, Terahertz band: Next frontier for wireless communications, *Phys. Commun.* **12** (2014) 16–32.
8. M. Tonouchi, Cutting-edge terahertz technology, *Nat. Photonics* **1** (2007) 97–105.
9. S. Koenig, D. Lopez-Diaz, J. Antes, F. Boes, R. Henneberger, A. Leuther, A. Tessmann, R. Schmogrow, D. Hillerkuss, R. Palmer, T. Zwick, C. Koos, W. Freude, O. Ambacher, J. Leuthold and I. Kallfass, Wireless sub-THz communication system with high data rate, *Nat. Photonics* **7** (2013) 977–981.
10. H. J. Song and T. Nagatsuma, Present and future of terahertz communications, *IEEE Trans. Terahertz Sci. Technol.* **1** (2011) 256–263.
11. A. Maestrini, I. Mehdi, J. V. Siles, J. S. Ward, R. Lin, B. Thomas, C. Lee, J. Gill, G. Chattopadhyay, J. Pearson and P. Siegel, Design and characterization of a room temperature all-solid-state electronic source tunable from 2.48 to 2.75 THz, *IEEE Trans. Terahertz Sci. Technol.* **2** (2012) 177–185.
12. J. Zhao, Z. Zhu, W. Cui, K. Xu, B. Zhang, D. Ye, C. Li and L. Ran, Power synthesis at 110-GHz frequency based on discrete sources, *IEEE Trans. Microw. Theory Tech.* **63** (2015) 1633–1644.
13. C. H. Page, Harmonic generation with ideal rectifiers, *Proc. IRE* **46** (1958) 1738–1740.
14. S. H. Yang, M. R. Hashemi, C. W. Berry and M. Jarrahi, 7.5% Optical-to-terahertz conversion efficiency offered by photoconductive emitters with three-dimensional plasmonic contact electrodes, *IEEE Trans. Terahertz Sci. Technol.* **4** (2014) 575–581.
15. A. Q. Zhao and B. S. Yu, The nonlinear designs and experiments on a 0.42-THz second harmonic gyrotron with complex cavity, *IEEE Trans. Electron Devices* **42** (2017) 564–570.
16. J. H. Booske, R. J. Dobbs, C. D. Joye, C. L. Kory, G. R. Neil, G.-S. Park, J. Park and R. J. Temkin, Vacuum electronic high power terahertz sources, *IEEE Trans. Terahertz Sci. Technol.* **1** (2011) 54–75.
17. X. Yuan, W. Zhu, Y. Zhang, N. Xu, Y. Yan, J. Wu, Y. Shen, J. Chen, J. She and S. Deng, A fully-sealed carbon-nanotube cold-cathode terahertz gyrotron, *Sci. Rep.* **6** (2016) 32936.
18. S. I. Lepeshov, A. Gorodetsky, A. E. Krasnok, E. U. Rafailov and P. A. Belov, Enhancement of terahertz photoconductive antennas and photomixers operation by optical nanoantennas, *Laser Photonics Rev.* **11** (2017) 1600199, doi: 10.1002/lpor.201600199.

19. A. Yazgan, L. Jofre and J. Romeu, The state of art of terahertz sources: A communication perspective at a glance, *Proc. 40th Int. Conf. Telecommunications and Signal Processing* (2017).
20. S. Jameson and E. Socher, A 0.3 THz radiating active x27 frequency multiplier chain with 1 mW radiated power in CMOS 65-nm, *IEEE Trans. Terahertz Sci. Technol.* **5** (2015) 645–648.
21. J. Grzyb, Y. Zhao and U. R. Pfeiffer, A 288-GHz lens-integrated balanced triple-push source in a 65-nm CMOS technology, *IEEE J. Solid-State Circuits* **48** (2013) 1751–1761.
22. S. Jameson and E. Socher, High efficiency 293 GHz radiating source in 65 nm CMOS, *IEEE Microw. Wirel. Compon. Lett.* **24** (2014) 463–465.
23. Y. Yang, O. D. Gurbuz and G. M. Rebeiz, An eight-element 370–410-GHz phased-array transmitter in 45-nm CMOS SOI with peak EIRP of 8–8.5 dBm, *IEEE Trans. Microw. Theory Tech.* **64** (2016) 4241–4249.
24. X.-D. Deng, Y. Li, J. Li, C. Liu, W. Wu and Y. Z. Xiong, A 320-GHz 1×4 fully integrated phased array transmitter using 0.13-μm BiCMOS technology, *IEEE Trans. Terahertz Sci. Technol.* **5** (2015) 930–940.
25. A. H. M. Shirazi, A. Nikpaik, S. Mirabbasi and S. Shekhar, A quad-core-coupled triple-push 295-to-301 GHz source with 1.25 mW peak output power in 65 nm CMOS using slow-wave effect, *Proc. IEEE Radio Frequency Integrated Circuits Symp.* (2016), pp. 190–193.
26. M. Adnan and E. Afshari, 14.8 A 247-to-263.5GHz VCO with 2.6mW peak output power and 1.14% DC-to-RF efficiency in 65nm bulk CMOS, *Proc. IEEE Int. Solid-State Circuits Conf.* (2014), pp. 262–263.
27. T. Chi, J. Luo, S. Hu and H. Wang, A multi-phase sub-harmonic injection locking technique for bandwidth extension in silicon-based THz signal generation, *IEEE J. Solid-State Circuits* **50** (2015) 1861–1873.
28. S. S. Iyer, G. L. Patton, J. M. C. Stork, B. S. Meyerson and D. L. Harame, Heterojunction bipolar transistors using Si-Ge alloys, *IEEE Trans. Electron Devices* **36** (1989) 2043–2064.
29. J. Yun, J. Kim and J.-S. Rieh, A 280-GHz 10-dBm signal source based on InP HBT technology, *IEEE Microw. Wirel. Compon. Lett.* **27** (2017) 159–161.
30. S. Shopov, A. Balteanu, J. Hasch, P. Chevalier, A. Cathelin and S. P. Voinigescu, A 234–261-GHz 55-nm SiGe BiCMOS signal source with 5.4–7.2 dBm output power, 1.3% DC-to-RF efficiency, and 1-GHz divided-down output, *IEEE J. Solid-State Circuits* **51** (2016) 2054–2065.
31. H.-C. Lin and G. M. Rebeiz, A SiGe multiplier array with output power of 5–8 dBm at 200–230 GHz, *IEEE Trans. Microw. Theory Tech.* **64** (2016) 2050–2058.
32. J. Yun, D. Yoon, S. Jung, M. Kaynak, B. Tillack and J. S. Rieh, Two 320 GHz signal sources based on SiGe HBT technology, *IEEE Microw. Wirel. Compon. Lett.* **25** (2015) 178–180.
33. R. Han, C. Jiang, A. Mostajeran, M. Emadi, H. Aghasi, H. Sherry, A. Cathelin and E. Afshari, A SiGe terahertz heterodyne imaging transmitter with 3.3 mW radiated power and fully-integrated phase-locked loop, *IEEE J. Solid-State Circuits* **50** (2015) 2935–2947.
34. H. Aghasi, A. Cathelin and, E. Afshari, A 0.92-THz SiGe power radiator based on a nonlinear theory for harmonic generation, *IEEE J. Solid-State Circuits* **52** (2017) 406–422.
35. M. Seo, M. Urteaga, J. Hacker, A. Young, Z. Griffith, V. Jain, R. Pierson, P. Rowell, A. Skalare, A. Peralta, R. Li, D. Lin and M. Rodwell, InP HBT IC technology for terahertz frequencies: Fundamental oscillators up to 0.57 THz, *IEEE J. Solid-State Circuits* **46** (2011) 2203–2214.
36. J. Yun, D. Yoon, H. Kim and J. S. Rieh, 300-GHz InP HBT oscillators based on common-base cross-coupled topology, *IEEE Trans. Microw. Theory Tech.* **62** (2014) 3053–3064.

37. J. Yun, S. J. Oh, K. Song, D. Yoon, H. Y. Son, Y. Choi, Y. M. Huh and J. S. Rieh, Terahertz reflection-mode biological imaging based on InP HBT source and detector, *IEEE Trans. Terahertz Sci. Technol.* **7** (2017) 274–283.
38. B. S. Williams, Terahertz quantum-cascade lasers, *Nat. Photonics* **1** (2007) 517–525.
39. J. H. Kim, S. Jung, Y. Jiang, K. Fujita, M. Hitaka, A. Ito, T. Masahiro and M. A. Belkin, 1.9 THz difference-frequency generation in mid-infrared quantum cascade lasers with grating outcouplers, *Proc. Conf. Lasers and Electro-Optics: Science and Innovations 2017* (2017).
40. Q. Lu, D. Wu, S. Sengupta, S. Slivken and M. Razeghi, Room temperature continuous wave monolithic tunable THz sources based on highly efficient mid-infrared quantum cascade lasers, *Sci. Rep.* **6** (2016) 23595, doi: 10.1038/srep23595.
41. Y. Jiang, K. Vijayraghavan, S. Jung, A. Jiang, J. H. Kim, F. Demmerle, G. Boehm, M. C. Amann and M. A. Belkina, Spectroscopic study of terahertz generation in mid-infrared quantum cascade lasers, *Sci. Rep.* **6** (2016) 21169, doi: 10.1038/srep21169.
42. Y. Irimajiri, M. Kumagai, I. Morohashi, A. Kawakami, S. Nagano, N. Sekine, S. Ochiai, S. Tanaka, Y. Hanado, Y. Uzawa and I. Hosako, Precise evaluation of a phase-locked THz quantum cascade laser, *IEEE Trans. Terahertz Sci. Technol.* **6** (2016) 115–120.
43. H. Richter, M. G. Bär, S. G. Pavlov, A. D. Semenov, M. Wienold, L. Schrottke, M. Giehler, R. Hey, H. T. Grahn and H. W. Hübers, Performance of a compact, continuous-wave terahertz source based on a quantum-cascade laser, *Proc. Int. Conf. Infrared, Millimeter and Terahertz Waves* (2010).
44. L. Li, L. Chen, J. Zhu, J. Freeman, P. Dean, A. Valavanis, A. G. Davies and E. H. Linfield, Terahertz quantum cascade lasers with > 1 W output powers, *Electron. Lett.* **50** (2014) 309–311.
45. A. Albo and Y. V. Flores, Temperature-driven enhancement of the stimulated emission rate in terahertz quantum cascade lasers, *IEEE J. Quantum Electron.* **53** (2017) 2300105, doi: 10.1109/JQE.2016.2631899.
46. G. Xu, R. Colombelli, S. P. Khanna, A. Belarouci, X. Letartre, L. Li, E. H. Linfield, A. G. Davies, H. E. Beere and D. A. Ritchie, Efficient power extraction in surface-emitting semiconductor lasers using graded photonic heterostructures, *Nat. Commun.* **3** (2012) 952, doi: 10.1038/ncomms1958.
47. M. Kim, J. Lee, J. Lee and K. Yang, A 675 GHz differential oscillator based on a resonant tunneling diode, *IEEE Trans. Terahertz Sci. Technol.* **6** (2016) 512–516.
48. J. Lee, M. Kim and K. Yang, A 1.52 THz RTD triple-push oscillator with a μW-level output power, *IEEE Trans. Terahertz Sci. Technol.* **6** (2016) 336–340.
49. J. Wang, A. A. Khalidi, K. Alharbi, A. Ofiare, H. Zhou, E. Wasige and J. Figueiredo, High performance resonant tunneling diode oscillators as terahertz sources, *Proc. European Microwave Conf.* (2016), pp. 341–344.
50. M. Asada and S. Suzuki, Room-temperature oscillation of resonant tunneling diodes close to 2 THz and their functions for various applications, *J. Infrared Millim. Terahertz Waves* **137** (2016) 1185–1198.
51. S. Kitagawa, S. Suzuki and M. Asada, Wide frequency-tunable resonant tunnelling diode terahertz oscillators using varactor diodes, *Electron. Lett.* **52** (2016) 479–481.
52. S. Kitagawa, S. Suzuki and M. Asada, 650-GHz resonant-tunneling-diode VCO with wide tuning range using varactor diode, *IEEE Electron Device Lett.* **35** (2014) 1215–1217.
53. T. Maekawa, H. Kanaya, S. Suzuki and M. Asada, Oscillation up to 1.92 THz in resonant tunneling diode by reduced conduction loss, *Appl. Phys. Express* **9** (2016) 024101, doi: 10.7567/APEX.9.024101.

54. T. Maekawa, H. Kanaya, S. Suzuki and M. Asada, Frequency increase in terahertz oscillation of resonant tunnelling diode up to 1.55 THz by reduced slot-antenna length, *Electron. Lett.* **50** (2014) 1214–1216.
55. H. Kanaya, H. Shibayama, R. Sogabe, S. Suzuki and M. Asada, Fundamental oscillation up to 1.31 THz in resonant tunneling diodes with thin well and barriers, *Appl. Phys. Express* **5** (2012) 124101.
56. E. Wasige, K. H. Alharbi, A. Al-Khalidi, J. Wang, A. Khalid, G. C. Rodrigues and J. Figueiredo, Resonant tunnelling diode terahertz sources for broadband wireless communications, *Proc. SPIE* **10103** (2017) 101031J, doi: 10.1117/12.2256357.
57. N. T. Yardimci, S.-H. Yang, C. W. Berry and M. Jarrahi, High-power terahertz generation using large-area plasmonic photoconductive emitters, *IEEE Trans. Terahertz Sci. Technol.* **5** (2015) 223–229.
58. H. Tanoto, J. H. Teng, Q. Y. Wu, M. Sun, Z. N. Chen, S. A. Maier, B. Wang, C. C. Chum, G. Y. Si, A. J. Danner and S. J. Chua, Greatly enhanced continuous-wave terahertz emission by nano-electrodes in a photoconductive photomixer, *Nat. Photonics* **6** (2012) 121–126.
59. S. H. Yang, R. Watts, X. Li, N. Wang, V. Cojocaru, J. O'Gorman, L. Barry and M. Jarrahi, High-performance terahertz source based on a bimodal laser diode and a plasmonic photomixer, *Proc. Int. Conf. Infrared, Millimeter, and Terahertz waves* (2016), pp. 1–2.
60. C. W. Berry, N. Wang, M. R. Hashemi, M. Unlu and M. Jarrahi, Significant performance enhancement in photoconductive terahertz optoelectronics by incorporating plasmonic contact electrodes, *Nat. Commun.* **4** (2013) 1622, doi: 10.1038/ncomms2638.
61. M. Jarrahi and T. H. Lee, High-power tunable terahertz generation based on photoconductive antenna arrays, *Proc. IEEE MTT-S Int. Microwave Symp.* (2008), pp. 391–394.
62. M. Scheller, J. M. Yarborough, J. V. Moioney, M. Fallahe, M. Koch and S. W. Koch, Continuous wave intracavity terahertz source, *Proc. European Quantum Electronics Conf.* (2011), doi: 10.1109/CLEOE.2011.5942527.
63. K. Moon, M. Lee, J. H. Shin. E. S. Lee, N. Kim, W. H. Lee, H. Ko, S. P. Han and K. H. Park, Bias field tailored plasmonic nanoelectrode for high-power terahertz photonic devices, *Sci. Rep.* **5** (2015) 13817, doi: 10.1038/srep13817.
64. N. Khiabani, Y. Huang, Y.-C. Shen and S. J. Boyes, Theoretical modeling of a photoconductive antenna in a terahertz pulsed system, *IEEE Trans. Antennas Propag.* **61** (2013) 1538–1546.
65. S. H. Yang and M. Jarrahi, A high-power photomixer with plasmonic contact electrodes, *Proc. 2016 Conf. Lasers and Electro-Optics* (2016).
66. N. T. Yardimci and M. Jarrahi, 1550 nm Large-area plasmonic photoconductive terahertz sources, *Proc. Conf. Lasers and Electro-Optics* (2016).
67. D. Turan, S. C. Corzo-Garcia, N. T. Yardimci, E. Castro-Camus and M. Jarrahi, Impact of the metal adhesion layer on the radiation power of plasmonic photoconductive terahertz sources, *J. Infrared Millim. Terahertz Waves* **38** (2017) 1448–1456, doi: 10.1007/s10762-017-0431-9.
68. N. T. Yardimci, S. Cakmakyapan, S. Hemmati and M. Jarrahi, A high-power broadband terahertz source enabled by three-dimensional light confinement in a plasmonic nanocavity, *Sci. Rep.* **7** (2017) 4166, doi: 10.1038/s41598-017-04553-4.
69. H. Murakami, S. Fujiwara, I. Kawayama and M. Tonouchi, Study of photoexcited-carrier dynamics in GaAs photoconductive switches using dynamic terahertz emission microscopy, *Photonics Res.* **4** (2016) A9–A15.
70. T. Wang, Z. Yang, S. Zou, K. Wang, S. Wang and J. Liu, Time behavior of field screening effects in small-size GaAs photoconductive terahertz antenna, *Front. Optoelectron.* **8** (2015) 98–103.

71. K. J. Siebert, A. Lisauskas, T. Löffler and H. G. Roskos, Field screening in low-temperature-grown GaAs photoconductive antennas, *Jpn. J. Appl. Phys.* **43** (2004) 1038–1043.
72. E. R. Brown, THz generation by photomixing in ultrafast photoconductors, *Int. J. High Speed Electron. Syst.* **13** (2003) 497.
73. M. Jarrahi, Advanced photoconductive terahertz optoelectronics based on nano-antennas and nano-plasmonic light concentrators, *IEEE Trans. Terahertz Sci. Technol.* **5** (2015) 391–397.
74. J. Y. Lee *et al.*, Near-field focusing and magnification through self-assembled nanoscale spherical lenses, *Nature* **460** (2009) 498–501.
75. G. V. Eleftheriades, EM transmission-line materials, *Mater. Today* **12** (2009) 30–41.
76. M. J. Steel, B. Marks and A. Rahmani, Properties of sub-diffraction limited focusing by optical phase conjugation, *Opt. Express* **18** (2010) 1487–1500.
77. A. Tuniz, K. J. Kaltenecker, B. M. Fischer, M. Walther, S. C. Fleming, A. Argyros and B. T. Kuhlmey, Metamaterial fibres for subdiffraction imaging and focusing at terahertz frequencies over optically long distances, *Nat. Commun.* **4** (2013) 2706, doi: 10.1038/ncomms3706.
78. J. Ma, N. J. Karl, S. Bretin, G. Ducournau and D. M. Mittleman, Frequency-division multiplexer and demultiplexer for terahertz wireless links, *Nat. Commun.* **8** (2017) 729, doi: 10.1038/s41467-017-00877-x.
79. K. M. Luk, S. F. Zhou, Y. J. Li, F. Wu, K. B. Ng, C. H. Chan and S. W. Pang, A microfabricated low-profile wideband antenna array for terahertz communications, *Sci. Rep.* **7** (2017) 1268, doi: 10.1038/s41598-017-01276-4.
80. H. Li, W. J. Wan, Z. Y. Tan, Z. L. Fu, H. X. Wang, T. Zhou, Z. P. Li, C. Wang, X. G. Guo and J. C. Cao, 6.2-GHz modulated terahertz light detection using fast terahertz quantum well photodetectors, *Sci. Rep.* **7** (2017) 3452, doi: 10.1038/s41598-017-03787-6.
81. S. J. Kindness, D. S. Jessop, B. Wei, R. Wallis, V. S. Kamboj, L. Xiao, Y. Ren, P. B. Weimer, A. I. Aria, S. Hofmann, H. E. Beere, D. A. Ritchie and R. D. Innocenti, External amplitude and frequency modulation of a terahertz quantum cascade laser using metamaterial/graphene devices, *Sci. Rep.* **7** (2017) 7657, doi: 10.1038/s41598-017-07943-w.
82. X. L. Tang, Q. Zhang, S. Hu, Y. Zhuang, A. Kandwal, G. Zhang and Y. Chen, Continuous beam steering through broadside using asymmetrically modulated Goubau line leaky-wave antennas, *Sci. Rep.* **7** (2017) 11685, doi: 10.1038/s41598-017-12118-8.
83. I. F. Akyildiz and J. M. Jornet, Realizing ultra-massive mimO (1024×1024) communication in the (0.06-10) terahertz band, *Nano Commun. Netw.* **8** (2016) 46–54.
84. A. Acharyya and J. P. Banerjee, Prospects of IMPATT devices based on wide bandgap semiconductors as potential terahertz sources, *Appl. Nanoscience* **4** (2014) 1–14.
85. T. Takahashi, Y. Kawano, K. Makiyama, S. Shiba, M. Sato, Y. Nakasha and N. Hara, Enhancement of $f_{\max}$ to 910 GHz by adopting asymmetric gate recess and double-side-doped structure in 75-nm-gate InAlAs/InGaAs HEMTs, *IEEE Trans. Electron Devices* **64** (2017) 89–95.
86. S. Bouzid-Driad, H. Maher, N. Defrance, V. Hoel, J.-C. De Jaeger, M. Renvoise and P. Frijlink, AlGaN/GaN HEMTs on silicon substrate with 206-GHz $F_{\max}$, *IEEE Electron Device Lett.* **34** (2013) 36–38.
87. Y. Tang, K. Shinohara, D. Regan, A. Corrion, D. Brown, J. Wong, A. Schmitz, H. Fung, S. Kim and M. Micovic, Ultrahigh-speed GaN high-electron-mobility transistors with $f_T/f_{\max}$ of 454/444 GHz, *IEEE Electron Device Lett.* **36** (2015) 549–551.